Redox Biology 45 (2021) 102031

Contents lists available at ScienceDirect

Redox Biology

journal homepage: www.elsevier.com/locate/redox

Peroxidasin promotes diabetic vascular endothelial dysfunction induced by advanced glycation end products via NOX2/HOCl/Akt/eNOS pathway

Jing Cao [a], Guogang Zhang [a,f], Zhaoya Liu [c], Qian Xu [d], Chan Li [b], Guangjie Cheng [e], Ruizheng Shi [b,f,*]

[a] Department of Cardiovascular Medicine, The Third Xiangya Hospital of Central South University, 410013, Changsha, China
[b] Department of Cardiovascular Medicine, Xiangya Hospital, Central South University, 41008, Changsha, China
[c] Department of Geriatrics, The Third Xiangya Hospital of Central South University, 410013, Changsha, China
[d] Department of Cardiothoracic Surgery, Xiangya Hospital, Central South University, 410008, Changsha, China
[e] Division of Pulmonary, Allergy & Critical Care Medicine, Department of Medicine, University of Alabama at Birmingham, Birmingham, 35294, AL, USA
[f] National Clinical Research Center for Geriatric Disorders, Xiangya Hospital, Central South University, Changsha, Hunan, 410008, China

ARTICLE INFO

Keywords:
Peroxidasin (PXDN)
Endothelial dysfunction
Advanced glycation end products (AGEs)
Endothelium nitric oxide synthase (eNOS)
Nicotinamide adenine dinucleotide phosphate (NADPH) oxidase
Reactive oxygen species (ROS)

ABSTRACT

Reactive oxygen species (ROS) derived from NADPH oxidases (NOX) plays an essential role in advanced glycation end products (AGEs)-induced diabetic vascular endothelial dysfunction. Peroxidasin (PXDN, VPO1) is one member of peroxidases family that catalyzes hydrogen peroxide (H_2O_2) to hypochlorous acid (HOCl). This present study aimed to elucidate the role of PXDN in promoting vascular endothelial dysfunction induced by AGEs in diabetes mellitus. We found that, compared to non-diabetic (db/m) mice, PXDN expression was notably increased in db/db mice with impaired endothelium-dependent relaxation. Knockdown of PXDN in vivo through tail vein injection of siRNA restored the impaired endothelium-dependent relaxation function of db/db mice which is accompanied with up-regulation of eNOS Ser1177 phosphorylation and NO production. AGEs significantly elevated expression of PXDN and 3-Cl-Tyr, but decreased phosphorylation of Akt and eNOS and NO release in HUVECs. All these effects induced by AGEs were remarkable alleviated by silencing PXDN with small interfering RNAs. In addition, HOCl treatment alone as well as HOCl added with Akt inhibitor MK2206 inhibited phosphorylation of Akt and eNOS, reducing NO production. More importantly,AGEs-induced up-regulation of PXDN and 3-Cl-Tyr with endothelial dysfunction were transformed by NOX2 silencing and H_2O_2 scavengers. Thus, these results support the conclusion that PXDN promotes AGEs-induced diabetic vascular endothelial dysfunction by attenuating eNOS phosphorylation at Ser1177 via NOX2/HOCl/Akt pathway.

1. Introduction

Vascular complications as a result of diabetes mellitus (DM) currently poses a significant public health risk in the world, as nearly 75% of diabetic patients die of vascular disease [1,2]. The intima of blood vessels is comprised of an endothelial barrier that maintains physiological homeostasis by releasing molecules. Vasoconstriction stimulus such as noradrenaline, thrombin and hypoxia, triggers endothelial nitric oxide synthase (eNOS) to produce nitric oxide (NO), and promotes vascular tone relaxation [3,4]. Many studies reported hyperglycemia, insulin resistance, advanced glycation end products (AGEs) and its receptor RAGE inhibit eNOS activity, reduce NO production, promote endothelial dysfunction and eventually lead to the occurrence of diabetic vascular disease [5–7].

Under a prolonged state of hyperglycemia, non-enzymatic glycation or glycoxidation of proteins, lipids, and nucleic acids induced AGEs and reactive oxygen species (ROS) accumulation in endothelium, which contributes to diabetic endothelial dysfunction [8]. ROS that generated from mitochondrial and especially NADPH oxidase 2 (NOX2) in endothelial cells inhibits eNOS activity by promoting eNOS uncoupling and decreasing phosphorylation of eNOS [9–11]. However, the exact mechanism of how AGEs/NOX2/ROS regulate eNOS activity remains unknown.

Peroxidasin (PXDN) was firstly reported in Drosophila by Nelson et al. [12] and plays an important role in ocular development [13,14]. In

* Corresponding author. Department of Cardiovascular Medicine, Xiangya Hospital, Central South University, 41008, Changsha, China.
E-mail addresses: 479328353@qq.com (Jing Cao), zhangguogang@csu.edu.cn (G. Zhang), 527269518@qq.com (Z. Liu), 21905078@qq.com (Q. Xu), 838022561@qq.com (C. Li), gjcheng@uab.edu (G. Cheng), xyshiruizheng@csu.edu.cn (R. Shi).

https://doi.org/10.1016/j.redox.2021.102031
Received 21 December 2020; Received in revised form 14 May 2021; Accepted 31 May 2021
Available online 6 June 2021

Abbreviations

3-Cl-Tyr	3-Chlorotyrosine
4-HNE	4-Hydroxynonenal
Ach	Acetylcholine
AGEs	Advanced glycation end products
ALT-711	Alagebrium
eNOS	Endothelial nitric oxide synthase
FBS	Fetal bovine serum
GAPDH	Glyceraldehyde-3-phosphate dehydrogenase
HbAlc	Glycosylated hemoglobin
HUVECs	Human umbilical vein endothelial cells
MDA	Malondialdehyde
NO	Nitric oxide
NOX1	NADPH oxidase 1
NOX2	NADPH oxidase 2
NOX4	NADPH oxidase 4
PXDN	Peroxidasin
RAGE	Receptor for advanced glycation end products
ROS	Reactive oxygen species
SNP	sodium nitroprusside.

2008, PXDN was renamed vascular peroxidase1 (VPO1) for the reason of detecting highly expressed in the cardiovascular system including endothelial cells, vascular smooth muscle cells, cardiomyocytes as well as extracellular matrix [15–19]. PXDN generates hypohalous acids (HOCl) by catalyzing hydrogen peroxide (H_2O_2), which aggravates oxidative stress in vasculature [20,21]. We have previously reported that PXDN decreases eNOS expression in response to angiotensin II [17]. However, the role of PXDN in diabetic endothelial dysfunction was unclear.

Here we reported for the first time that PXDN promotes diabetic vascular endothelial dysfunction through the NOX2/HOCl/Akt/eNOS pathway induced by AGEs.

2. Materials and methods

Refer to supplementary materials for detailed methods.

2.1. Animal

Experiments were conducted in accordance with the National Institutes of Health Guide for the Care and Use of Laboratory Animals, and all experimental protocols were approved by the Medicine Animal Welfare Committee of the Third Xiangya Hospital of Central South University (Approval NO: 201703121; Changsha, China). 11-week-old male db/db mice with a C57BLKS/JNju background (db/db; BKS.Cg-Dock7$^{m\ +/+}$ Lepr^{db}/J) and control db/m mice with the same background were obtained from Model Animal Research Center of Nanjing University (Nanjing, China).

2.2. Metabolic parameters test

Body weights of mice were measured using an electronic scale (PL6001E, Mettler Toledo, Zurich, Switzerland). Blood glucose was assessed in random-fed status mice using a glucometer (SAFE-ACCU, Sinocare Inc, Changsha, China) to analyze blood samples collected from tail veins. Glycosylated hemoglobin (HbAlc) and other serum biochemical markers were evaluated by assay kit according to the manufacturer's protocol.

2.3. Measurement of vascular function

Endothelium-dependent and endothelium-independent relaxation of the mice thoracic aortas in response to acetylcholine (ACh) and sodium nitroprusside (SNP), respectively, were assessed as previously described [22–24].

2.4. Cell culture and experiments

Human umbilical vein endothelial cells (HUVECs) were obtained from ScienCell Research Laboratories (San Diego, CA, USA). HUVECs were cultured in endothelial cell medium (ScienCell Research Laboratories, CA, USA) with 5% fetal bovine serum (FBS) and 1% endothelial cell growth supplement (ECGS) at 37 °C and 5% CO_2. For experiments, cells were used between passages 3 and 8.

2.5. Western blot analysis

Isolated thoracic aortic tissues or cultured HUVECs were lysed in commercially purchased RIPA lysis buffer (P0013B, Beyotime, Shanghai, China) spiked with 1 mmol/L phenylmethanesulfonyl fluoride (ST506, Beyotime, Shanghai, China) to obtain protein products. The antibodies against the following proteins were used: PXDN (1 μg/mL, ABS1675, Merck, Frankfurter, Germany), RAGE (0.3 μg/mL, ab37647, Abcam, Cambridge, UK), NOX2 (0.25 μg/mL, ab80508, Abcam, Cambridge, UK), NOX1 (0.5 μg/mL, ab131088 and ab121009, Abcam, Cambridge, UK), NOX4 (0.33 μg/mL, ab154244, Abcam, Cambridge, UK), 3-chlorotyrosine (0.1 μg/mL, 3-Cl-Tyr, HP5002, Hycult biotech, Uden, Netherlands), 4-hydroxynonenal (0.43 μg/mL, 4-HNE, ab46545, Abcam, Cambridge, UK), Akt (0.5 μg/mL, SAB4500797, Sigma-Aldrich, USA), p-Akt (0.143 μg/mL, ab18206, Abcam, Cambridge, UK), eNOS (0.25 μg/mL, 61029, BD, Biosciences, NJ, USA) and p-eNOS (0.056 μg/mL dilution, Ser1177, MA5-14957, Invitrogen, CA, USA). Expression of the protein GAPDH (0.5 μg/mL, SAB1405848, Sigma-Aldrich, MO, USA) was used for data normalization. PVDF membranes were incubated with a horseradish peroxidase linked secondary antibody and bands were visualized using gel documentation system (Bio-Rad).

2.6. Immunofluorescence staining

Cryosection of thoracic aortas and mesenteric arteries were blocked in 5% bovine serum albumin (BSA, A1933, Sigma-Aldrich, MO, USA) diluted in phosphate buffered saline (PBS) for 1 h at room temperature and subsequently incubated with goat anti-PXDN (10 μg/mL, sc-168598, Santa Cruz, TX, USA) and rabbit anti-CD31 (1:20 dilution, ab28364, Abcam, Cambridge, UK), anti-RAGE (1 μg/mL, ab37647, Abcam, Cambridge, UK) and anti-3chlorotyrosine (2 μg/mL, HP5002, Hycult biotech, Uden, Netherlands) antibodies overnight at 4 °C in a humidity box. Samples were then incubated with secondary antibody for 1 h at room temperature. Finally, DAPI (5 μg/mL, D9542, Sigma-Aldrich, MO, USA) was used for nuclear staining.

2.7. Detection of superoxide

Intracellular superoxide levels were evaluated by Dihydroethidium (DHE) fluorescence probe. For thoracic aortas and mesenteric arteries, cryosection were incubated with DHE (Ex518/Em606 nm, 5 μmol/L; D23107, Invitrogen)-containing PBS at 37 °C for 15 min. For HUVECs, cells were seeded in the six-well plates and incubated with DHE in PBS at 37 °C for 30 min. Fluorescence image were obtained with a fluorescence microscopy (Eclipse, Nikon, Japan) and analyzed by measuring the fluorescence intensity.

2.8. Assessment of NO production

The level of NO in plasma and cell supernatants was indirectly

determined by Total Nitric Oxide Assay Kit (S0024, Beyotime, Shanghai, China) which measures the concentration of nitrate and nitrite by Griess assay. The optical densities at 540 nm wavelength were recorded using a Multimode Detector (DTX 880, Beckman Coulter, CA, USA) and the concentrations of NO were calculated according to the standard curve.

2.9. Statistical analysis

All data were presented as mean ± SEM. Concentration–response curves were analyzed by nonlinear regression curve fitting using GraphPad Prism 8.0 software followed by two-way ANOVA and Student–Newman–Keuls post-hoc testing. Whether the data is consistent with normally distributed and equal variance were evaluated using Kolmogorov-Smirnov and Levene's test before statistical comparisons. Data of normally distributed was detected by T-test or ANOVA, otherwise tested by non-parametric test. Unpaired Student's t-test or Mann–Whitney *U* test was used for two experimental groups and one-way ANOVA or Kruskal-Wallis H test were used for multiple groups. Post-hoc comparisons were performed using Student–Newman–Keuls or Dunnett's Test. A two-tailed value of $p < 0.05$ was considered statistically significant. Statistics were done using GraphPad Prism 8.0 and SPSS 22.0.

3. Results

3.1. PXDN expression is elevated in db/db mice with impaired endothelium-dependent relaxation

The db/db mice were used as diabetic animal model and the db/m were used as the control in this study. Body weight, fasting blood glucose, HbA1c and other serum biochemical markers were measured and described in supplementary table 1. Vascular functions of mice were evaluated by measuring dilatory responses of pressurized thoracic aortas to vasoactive agents. Endothelium-dependent relaxations in response to Ach were impaired by 62.50% ($p < 0.01$) in db/db mice compared with db/m mice (Fig. 1A), while no significant difference in SNP-induced endothelium-independent relaxation was observed (Fig. 1B). Moreover, the NO production in plasma was significantly decreased in db/db mice compared to db/m mice (29.03 ± 7.91 μmol/L vs 61.68 ± 12.09 μmol/L, $p < 0.01$, Fig. 1C). The expression of RAGE, PXDN, 3-Cl-Tyr (a surrogate measure of HOCl production), *p*-eNOS, *p*-Akt, NOX1, 2, 4, and the levels of H_2O_2, superoxide, oxidative stress products (4-hydroxynonenal (4-HNE) and malondialdehyde (MDA)) were measured by Western blot, fluorescence probe or kits. We found that RAGE protein expression was elevated (Fig. 1D and Figure S1A) in aortas of db/db mice compared to db/m mice. The protein expression of NOX family (NOX1, 2 and 4) was up-regulated in thoracic aortas from db/db mice compared with the db/m group, and the increase of NOX2 was more obvious than NOX1 and NOX4 (Fig. 1D, Figure S1D-F). The ROS level including H_2O_2, superoxide, 4-HNE and MDA was up-regulated concurrently in diabetic mice (Fig. 1H, G, K, E and I). ROS levels detected using DHE probe were inhibited by non-specific NOX inhibitor (VAS2870), specific NOX2 inhibitor (GSK2795039), and mitochondrial superoxide scavenger (Mito-TEMPO), while the effect of ROS attenuation treated with NOX2-specific inhibitor was more significant than that of non-specific NOX inhibitor and mitochondrial superoxide scavenger (Figure S1L-N). Furthermore, expression of PXDN and 3-Cl-Tyr in db/db mice was also obviously increased compared with the db/m (2.9-fold and 3.3-fold, respectively, Fig. 1F–J). Alternatively, the phosphorylation level of eNOS on Ser1177 in db/db mice was significantly decreased (Fig. 1D, Figure S1B). Although the protein expression of total eNOS was also decreased, while was no statistical difference ($p = 0.1238$, Figure S1C).

In the endothelium of both mesenteric arteries and thoracic aortas, the expression of PXDN in db/db mice was significantly increased and co-localized with CD31 (marker of endothelium) compared to db/m mice (Fig. 1G, Figure S1H and Figure S1I). Moreover, expression level of RAGE, 3-Cl-Tyr was also increased in the mesenteric artery and thoracic aortas endothelium of db/db animals (Fig. 1G, Figure S1J and K) compared to db/m mice.

3.2. Knockdown of PXDN attenuates AGEs induced endothelial dysfunction in db/db mice

To clarify the role of PXDN in AGEs induced diabetic endothelial dysfunction, PXDN siRNA and AGEs breaker (Alagebrium, ALT-711) were used in diabetic mice. After tail vein siRNA injection three times a week, mice were injected intraperitoneally with ALT-711 simultaneously until sacrificed at 12 weeks (Fig. 2A). Body weight, fasting blood glucose, HbA1c and other serum biochemical markers of mice were measured and summarized in Supplementary table 2. The knockdown efficiency of PXDN was detected by Western blot. As shown in Fig. 2G, PXDN expression was significantly inhibited after injection of PXDN siRNA in aortas of mice (78.6% reduction, $p < 0.01$). We further found that si-PXDN treatment significantly improved the Ach-induced aortic endothelium-dependent relaxation (64.67% vs 34.20%, Fig. 2B) and plasma NO level (44.35 ± 8.46 μmol/L vs 24.17 ± 6.85 μmol/L, Fig. 2F) compared to db/db mice, while without affecting the endothelium-independent relaxation responses to SNP (Fig. 2D). In addition, treatment with ALT-711 combined with si-PXDN in diabetic mice improved vascular function (Ach-induced relaxation: 66.97%; NO level: 50.11 ± 10.59 μmol/L), which was similar to the effect of si-PXDN but more significant than ALT-711 alone (Ach-induced relaxation: 47.45%; NO level: 38.36 ± 6.98 μmol/L) (Fig. 3D–F). Whereas all of these treatments did not alter vascular function in non-diabetic mice. ALT-711 treatment remarkedly inhibited RAGE, NOX2 expression and H_2O_2 production in the aortas of db/db mice (Fig. 2G and H and Figure S2A) while si-PXDN did not affect this change. PXDN and 3-Cl-Tyr level were declined significantly in db/db mice treated with ALT-711, si-PXDN or both, which accompanied with the reduce of superoxide and oxidative stress products 4-HNE and MDA (Fig. 2G–I, Fig. 3A–C and Figs. 3A and S3C). Moreover, the level of eNOS phosphorylation on Ser1177 in aortas of db/db mice was rescued after treated with ALT-711, si-PXDN or both. (Fig. 2G).

Researches show that PI3K/Akt pathway is involved in regulating endothelial eNOS phosphorylation and vasodilation [25–27]. In addition, we found that phosphorylation level of Akt on Ser473 in aortas of db/db mice was significantly decreased (Fig. 1D, Figure S1G). This reduction was recovered after PXDN knockdown (Figure S2B), which suggests that Akt may be involved in PXDN- mediated diabetic vascular endothelial dysfunction.

3.3. Knockdown of PXDN reduces HOCl and ROS levels in both microvascular and macrovascular endothelium of db/db mice

Diabetic endothelial dysfunction occurs more than in the macrovascular and also in microvessels such as the mesenteric artery. To further determine the effect of PXDN knockdown on different arteries, DHE and immunofluorescent staining was used to detect arterial superoxide and HOCl production after PXDN knockdown. As shown in Figure S4, superoxide levels were declined in mesenteric artery after db/db were treated with ALT-711, si-PXDN or both. Consistent with the results of Western blot, 3-Cl-Tyr protein expression was significantly decreased in the thoracic aortas of db/db mice treated with si-PXDN (Fig. 3B–D). In addition, si-PXDN combined with ALT-711 has more significant effect on reducing 3-Cl-Tyr protein expression than treated with ALT-711 alone in db/db mice (Figure S3B and S3D). Interestingly, these changes also appeared in the mesenteric artery, which was even more obvious (Fig. 3B–E, Figure S3B and S3E).

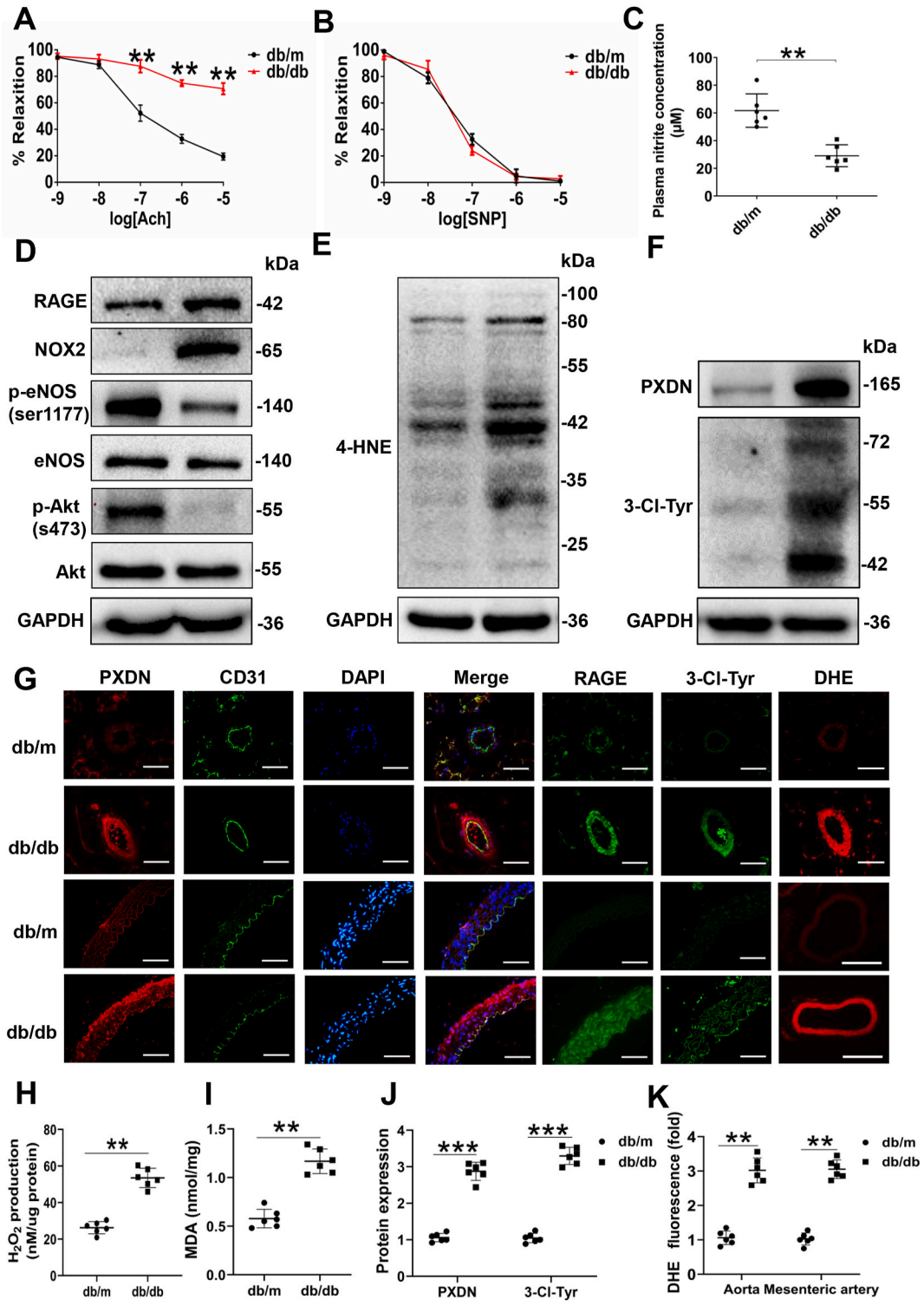

Fig. 1. PXDN expression is elevated in db/db mice with impaired endothelium-dependent relaxation. A and B, endothelium-dependent and endothelium-independent relaxation of thoracic aortic rings were assessed by vascular functional experiments; C, nitrite concentration in plasma was measured by Total Nitric Oxide Assay Kit; D, expression of RAGE, NOX2, *p*-eNOS^{Ser1177}/total eNOS and *p*-Akt^{Ser473}/total Akt in thoracic aortic tissues of db/db and db/m mice was measured by Western blot; E, expression 4-HNE in thoracic aortic tissues of db/db and db/m mice was measured by Western blot; F and J, expression of PXDN and 3-Cl-Tyr in thoracic aortic tissues of db/db and db/m mice was measured by Western blot and quantified by Image Lab software; H, H_2O_2 concentration of thoracic aortas was assessed by Hydrogen Peroxide Assay Kit; I, MDA concentration of thoracic aortas was measured by MDA kit; n = 6 mice for each group. Tissue superoxide level was measured by DHE staining, and expression of PXDN, 3-Cl-Tyr and RAGE in thoracic aortas and mesenteric arteries was measured by immunofluorescence staining. G, representative cross-sections of mesenteric arteries and thoracic aortas stained with DHE (red), PXDN (red), CD31 (green), RAGE (green), 3-Cl-Tyr (green) and DAPI (blue) in db/m and db/db mice; K, quantification of DHE staining fluorescence intensity within the thoracic aortic and mesenteric arterial endothelial layer; n = 6 mice for DHE staining; n = 3 mice for immunofluorescence staining. Data are expressed as the mean ± SEM. Bar = 500 μm for DHE staining of thoracic aortas and 50 μm for other fluorescence staining. Two-way ANOVA and Student–Newman–Keuls post-hoc testing was used for concentration–response curves. Unpaired Student's t-test was used for other comparison of compared groups. **p < 0.01, ***p < 0.001.

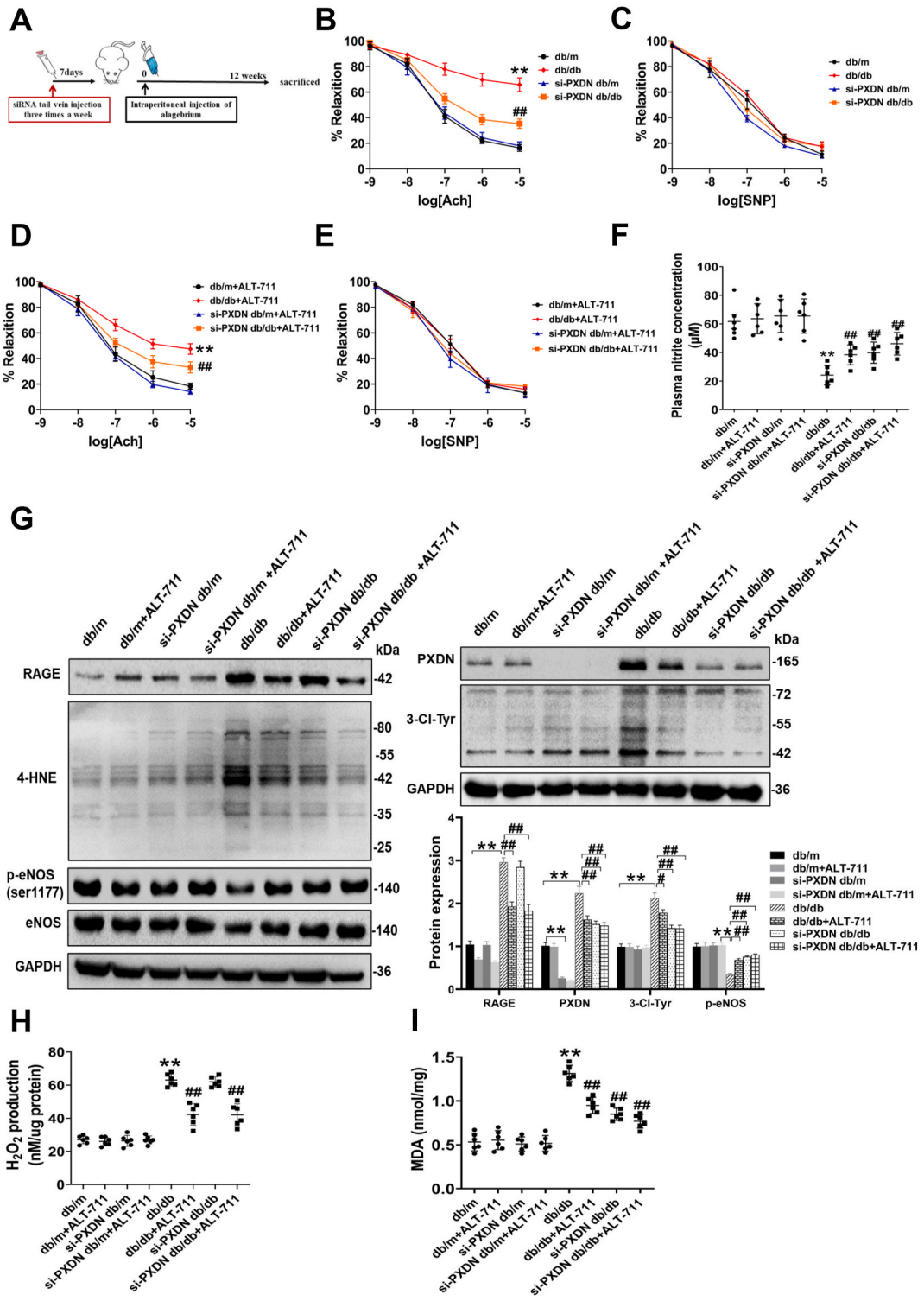

Fig. 2. Knockdown of PXDN attenuates AGEs induced endothelial dysfunction in db/db mice. A, experimental procedure for injecting siRNA, ALT-711 or both in mice; B-E, endothelium-dependent and endothelium-independent relaxation of thoracic aortic rings after mice received injections of siRNA, ALT-711 or both; F, Plasma nitrite concentration of db/m and db/db mice after received siRNA, ALT-711 or both injections was measured by Total Nitric Oxide Assay Kit; G, expression of RAGE, PXDN, 3-Cl-Tyr、4-HNE and *p*-eNOS^{Ser1177}/total eNOS in thoracic aortas was assessed by Western blot, and quantification of protein expression by Image Lab. H, H_2O_2 concentration of thoracic aortas was assessed by Hydrogen Peroxide Assay Kit; I: MDA concentration of thoracic aortas was measured by MDA kit. Data are expressed as the mean ± SEM (n = 6 for each group). Two-way ANOVA and Student–Newman–Keuls post-hoc testing were used for concentration–response curves. One-way ANOVA test followed by Student–Newman–Keuls or Kruskal-Wallis H followed by Dunnett's Test were used for other comparison of compared groups. **p < 0.01 versus db/m mice; $^{\#}$p < 0.05 versus db/db mice, $^{\#\#}$p < 0.01 versus db/db mice.

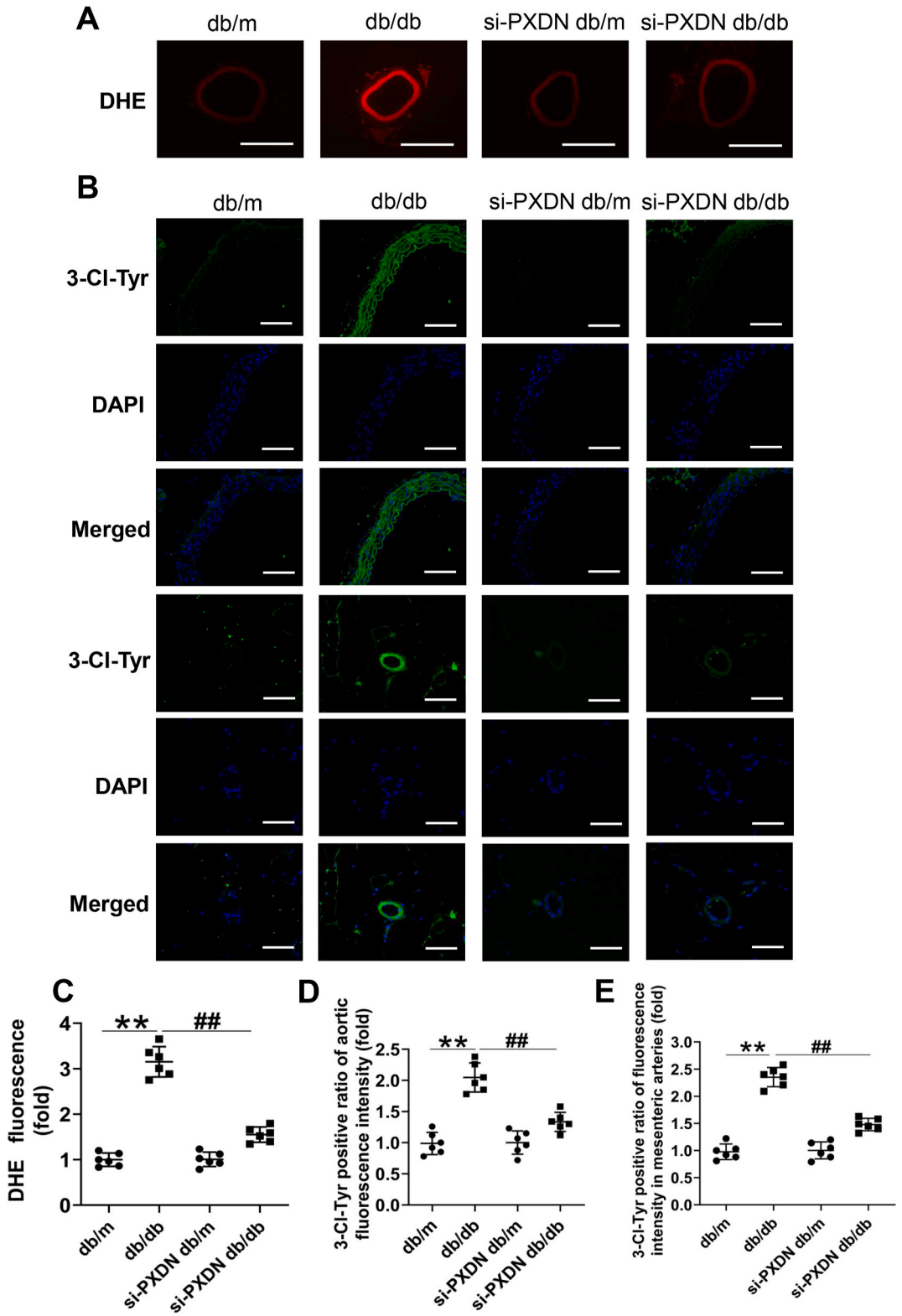

Fig. 3. Knockdown of PXDN reduces microvascular and macrovascular endothelial HOCl and ROS levels. A, representative cross-sections of thoracic aortas stained with DHE probe in db/m and db/db mice after injected with PXDN siRNA; B, representative cross-sections of thoracic aortas and mesenteric arteries stained with 3-Cl-Tyr (green) and DAPI (blue) in db/m and db/db mice after injected with PXDN siRNA. C, quantification of DHE staining fluorescence intensity within the thoracic aortic endothelial layer using Image J; D and E,quantification of microvascular and macrovascular 3-Cl-Tyr staining fluorescence intensity within the endothelial layer using Image J. Bar = 500 μm for DHE staining of thoracic aortas and 50 μm for other fluorescence staining. Data are expressed as the mean ± SEM (n = 6 mice for each group). One way-ANOVA followed by Student–Newman–Keuls test was used for compared groups. $^{**}p < 0.01$; $^{\#\#}p < 0.01$. (For interpretation of the references to colour in this figure legend, the reader is referred to the Web version of this article.)

3.4. AGE-BSA attenuates phosphorylation of eNOS and activates PXDN/HOCl pathways in cultured HUVECs

AGEs were used as a stimulus to mimic the pathologic state of diabetic endothelial dysfunction in vitro. As shown in Figure S5A and D, HUVECs were treated with AGE-BSA, protein expression of RAGE was up-regulated in a concentration-dependent and time-dependent manner. Inversely, phosphorylation level of eNOS on Ser1177 and Akt on Ser473 was reduced (Figure S5B, C E and F). In addition, the expression level of PXDN and 3-Cl-Tyr was increased (2.5-fold, Figure S5G; 2.3-fold, Figure S5I; 2.2-fold, S2H; 2.2-fold, Figure S5J). Moreover, the induction of PXDN expression peaked at 48 h after treatment with 200 μg/mL AGE-BSA.

3.5. PXDN silencing attenuates the effect of AGE-BSA on eNOS phosphorylation

To further explore the mechanism of PXDN regulating AGEs induced endothelial dysfunction, HUVECs were transfected with siRNA against PXDN. PXDN protein expression was successfully knocked down by PXDN-siRNA in HUVECs (75.0% reduction, $p < 0.01$, Figure S6A). The production of superoxide, oxidative stress products (MDA and 4-HNE) were significantly reduced in PXDN-siRNA transfection compared to the negative control siRNA transfected cells after treatment with AGEs, while the level of H_2O_2 was not affected (Fig. 4A–C and Figure S7A-C). In addition, expression of 3-Cl-Tyr was suppressed by si-PXDN after AGEs stimulation (Fig. 4D and E). Consistent with results of mice, PXDN silencing improved the reduction of Akt and eNOS phosphorylation (Fig. 4F and G) and NO level (20.72 ± 1.97 μmol/L vs 9.46 ± 2.23 μmol/L, Fig. 4H) upon AGE-BSA treatment.

3.6. HOCl reduces eNOS phosphorylation via phosphorylation of Akt

Previous studies have demonstrated that PXDN-derived HOCl exacerbates vascular oxidative stress [17,28]. To clarify this effect on endothelial dysfunction, HUVECs were incubated with different concentrations of HOCl (10 μmol/L and 100 μmol/L). HOCl treatment remarkably reduced phosphorylation of Akt on Ser473 and eNOS on Ser1177 (Fig. 5A and B). NO level was also reduced (10.78 ± 2.80 μmol/L vs 23.25 ± 2.48 μmol/L, Fig. 5E) in HOCl treated cells. Moreover, the effects of HOCl on eNOS phosphorylation and NO production (5.85 ± 1.87 μmol/L vs 11.69 ± 2.11 μmol/L) were aggravated by Akt specific inhibitor MK2206 (Fig. 5C, D and F).

3.7. H_2O_2, ROS scavengers and NOX inhibitors attenuate PXDN-mediated endothelial dysfunction induced by AGEs

PXDN is reported to aggravate NOX-mediated oxidative stress by utilizing chlorine and H_2O_2 to generate HOCl in endothelial cell apoptosis and smooth muscle cell proliferation [16,29]. To further explore the role of this mechanism in AGEs-induced endothelial dysfunction, H_2O_2 scavengers (PEG-catalase and ebselen), NOX inhibitors (VAS2870 and GSK2795039) and ROS scavenger (tempol) were used. We found that, H_2O_2 scavengers, NOX inhibitors and ROS scavenger decreased intracellular oxidative stress (Fig. 6A–C and Figure S7G-I). Moreover, these scavengers attenuated the induction of PXDN and 3-Cl-Tyr expression by AGEs (Fig. 6D and E), accompanied by the recovery of phosphorylation of Akt and eNOS (Fig. 6F and G) and NO production (20.14 ± 2.36 μmol/L, 18.93 ± 2.03 μmol/L, 20.54 ± 2.14 μmol/L, 21.85 ± 2.74 μmol/L and 18.31 ± 1.83 μmol/L vs 12.28 ± 2.15 μmol/L, Fig. 6H) in HUVECs.

3.8. NOX2 silencing attenuates the effect of AGE-BSA on PXDN and its downstream pathway, restoring endothelial function

Studies show that NOX2 play a critical role in AGEs-induced ROS production and endothelial dysfunction [30,31]. In the present study, we also observed a significant increase of NOX2 expression in the aortas of db/db mice (Fig. 1D). And NOX2-specific inhibitor had more significant effect on ROS attenuation than non-specific NOX inhibitor and mitochondrial ROS scavenger (Figure S1L-N),which suggested NOX2 may be a major source of ROS in diabetic mice. In order to elucidate whether NOX2 mediates PXDN in AGEs-induced endothelial dysfunction, NOX2 siRNA was used. NOX2 protein expression was successfully knocked down by NOX2-siRNA in HUVECs (80.4% reduction, $p < 0.01$, Figure S6B). Surprisingly, NOX2-siRNA transfection did not affect the expression of its family member NOX4 while decreased the level of NOX1 in HUVECs (Figure S8A and S8B). The results show that intracellular H_2O_2, superoxide, 4-HNE and MDA were declined with NOX2-siRNA transfection, compared to the control siRNA transfected cells treated with AGEs (Fig. 7A–C and Figure S7D-F). We also found the expression of PXDN and 3-Cl-Tyr was significantly down-regulated in the si-NOX2 transfected group after treated with AGEs compared with the control group (Fig. 7D and E). Additionally, NOX2 silencing improved phosphorylation reduction of Akt and eNOS (Fig. 7F and G) and NO level in cell supernatants (18.79 ± 2.42 μmol/L vs 10.59 ± 2.68 μmol/L, Fig. 7H) upon AGE-BSA treatment.

4. Discussion

Various clinical trials (ACCORD, ADVANCE and VADT Trials) have shown that diabetes-related vascular complications exist and even develop despite strict and long-term glycemic control [32–34]. AGEs are recognized as a key inductor for contributing to this phenomenon, while the mechanism remains unknown [35]. In the present study, we found that: (i) In db/db mice with impaired endothelial function, PXDN expression was increased. Knockdown of PXDN restored the impaired endothelium-dependent relaxation function of db/db mice, increased eNOS phosphorylation and NO production. (ii) In cultured HUVECs cells, PXDN silencing significantly inhibited AGEs-induced endothelial dysfunction, including improved eNOS phosphorylation on Ser1177 and NO production. (iii) The effect of PXDN on AGEs-induced endothelial dysfunction is mediated by NOX2/HOCl/Akt/eNOS pathway.

In diabetes with a prolonged state of hyperglycemia, AGEs were accumulated from the non-enzymatic glycation or glycoxidation of proteins, lipids, and nucleic acids. It is well-known that AGEs increase ROS by binding to RAGE and promote diabetic vascular endothelial dysfunction [36]. Myeloperoxidase (MPO), the heme-containing peroxidase highly expressed in leukocytes, is previously reported to leads to endothelial dysfunction by reducing the bioavailability of NO under inflammatory conditions of diabetic vascular disease, [37,38]. Unlike MPO, PXDN is highly expressed in the cardiovascular system including endothelial cell, vascular smooth muscle cell and extracellular matrix [18,29,39,40]. Moreover, as a secreted protein, the concentration of PXDN in plasma is 1000-fold higher than MPO [41]. It has been previously reported that PXDN catalyzes the oxidation of chloride in the presence of H_2O_2 to generate HOCl. The enzymatic function of PXDN plays a physiological role in participating in host immune against gram-negative bacterial pathogens [42,43], and was reported to aggravate NOX-mediated oxidative stress under pathological progress [16,29]. Multiple studies reported that PXDN contributes to pathological procedure of cardiovascular diseases such as vascular calcification, hypertension and cardiac hypertrophy [18,44,45]. Especially, our former researches have demonstrated that PXDN plays a key role in the endothelial cell senescence, apoptosis and endothelial progenitor cell dysfunction [46–50]. What's more, the preliminary research found that PXDN showed a significant function in regulating eNOS expression and activity [51]. These findings suggests that PXDN may be an important molecule in mediating AGEs-induced diabetic endothelial dysfunction. Here, we observed that the expression of PXDN and 3-Cl-Tyr was increased in the thoracic aortic and mesenteric arterial endothelium of db/db mice and AGEs-induced HUVECs cells. Knocking down of PXDN

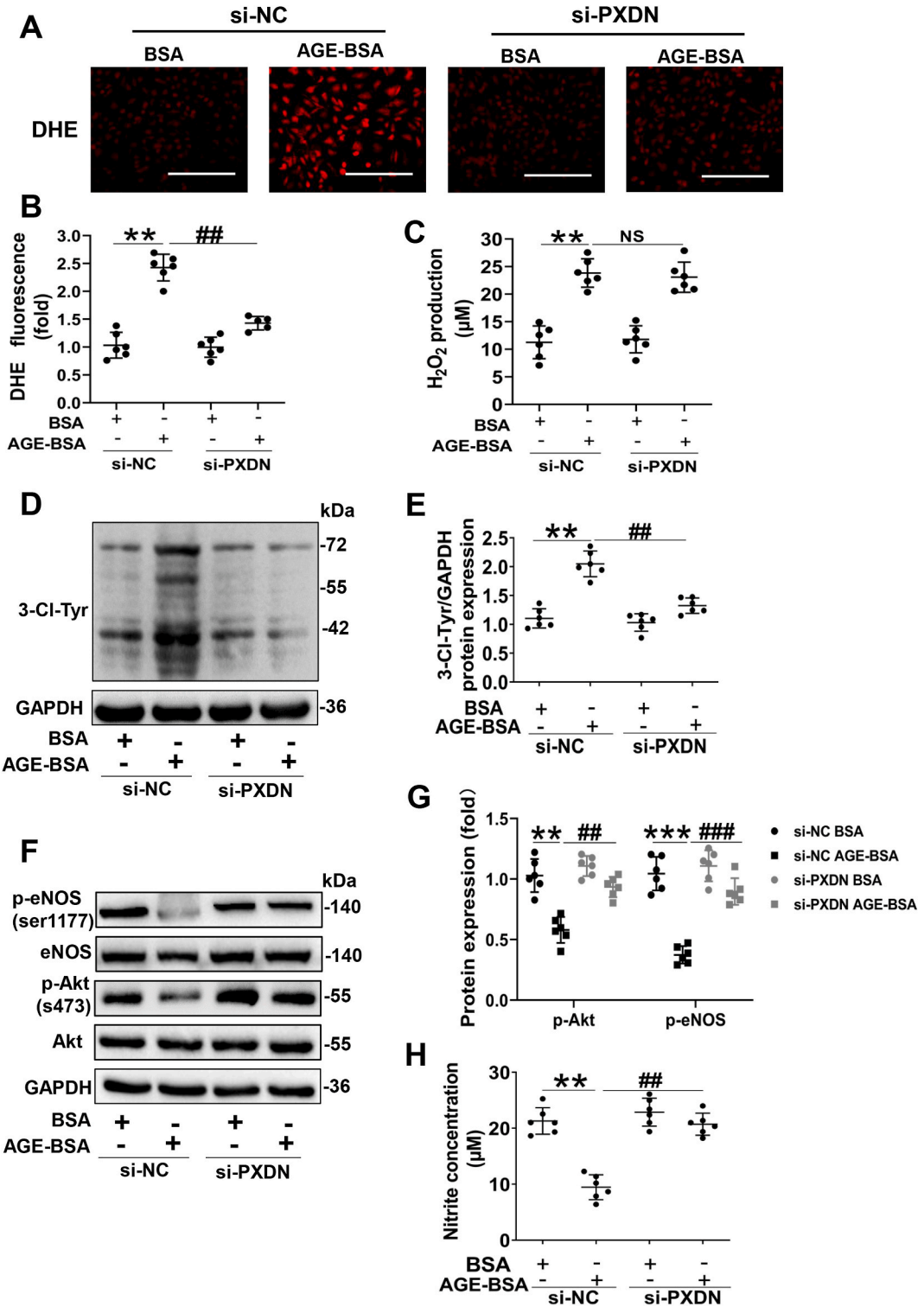

Fig. 4. PXDN silencing attenuates the effect of AGE-BSA on eNOS phosphorylation through HOCl/Akt pathway. Cells were transfected with either a negative control siRNA (si-NC) or PXDN siRNAs (si-PXDN) for 24 h. The medium was then replaced by endothelial cell medium containing 200 μg/mL AGE-BSA for 48 h. A, intracellular superoxide was measured using DHE staining; B, quantification of DHE staining fluorescence intensity by Image J; C, intracellular H_2O_2 concentration was assessed by Hydrogen Peroxide Assay Kit; D and E, cell expression level of 3-Cl-Tyr was measured by Western blot and quantified by Image Lab; F and G, phosphorylation level of *p*-Akt^{Ser473}/total Akt and *p*-eNOS^{Ser1177}/total eNOS was measured by Western blot and quantified by Image Lab; H, nitrite concentration in cell supernatants was measured by Total Nitric Oxide Assay Kit. Bar = 200 μm for DHE staining of HUVECs. Data are expressed as the mean ± SEM (n = 6 for each group). An ANOVA and a subsequent Student–Newman–Keuls test were conducted for this figure. $^{**}P < 0.01$ versus control, $^{**}p < 0.01$, $^{***}p < 0.001$; $^{\#\#}p < 0.01$, $^{\#\#\#}p < 0.001$; NS: not significant.

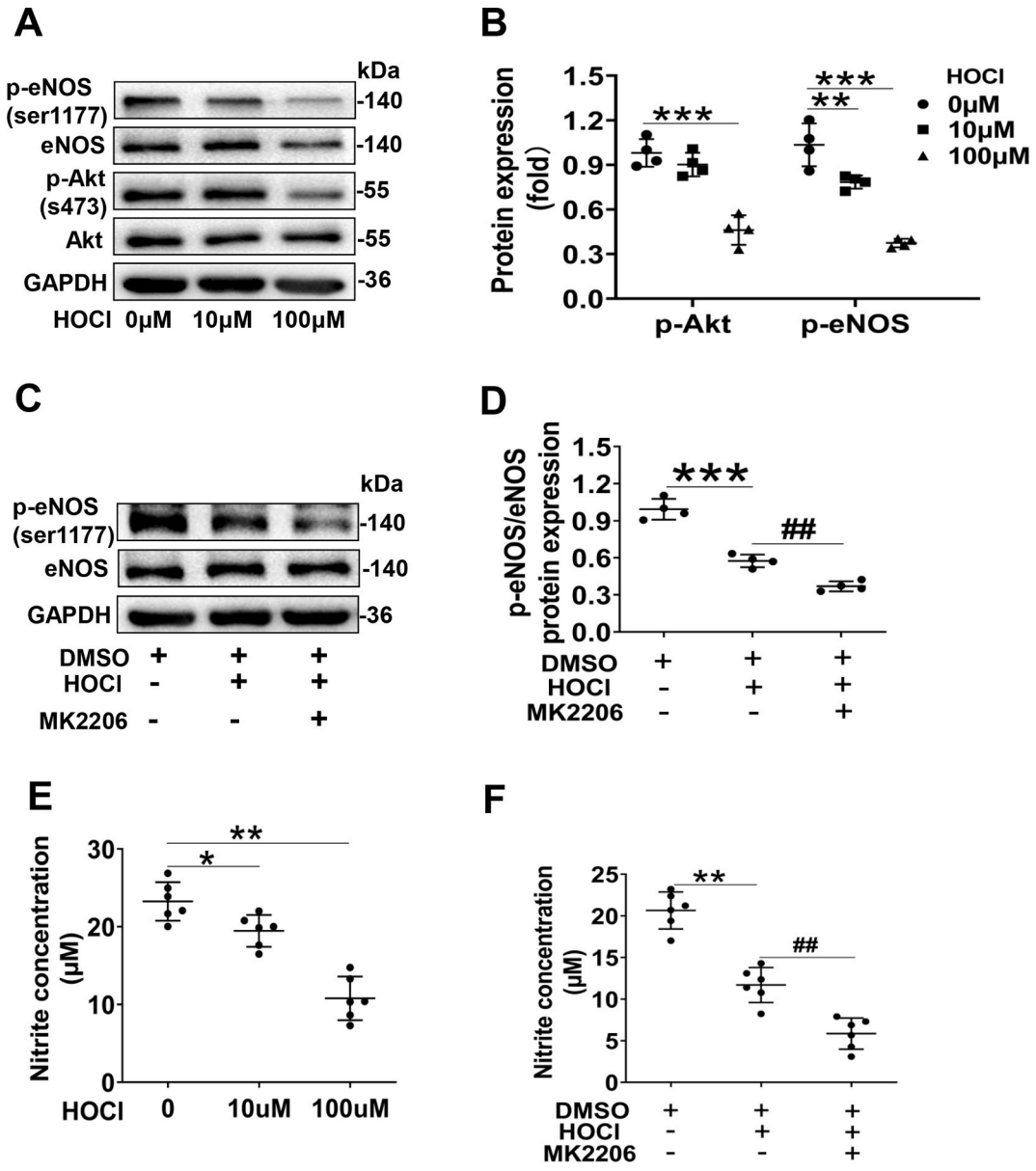

Fig. 5. HOCl reduces eNOS phosphorylation via Akt pathway. HUVECs were treated with 0, 10, 100 μmol/L HOCl for 2 h and allowed to recover for 24 h. A, Western blot to assess phosphorylation of *p*-Akt^{Ser473}/total Akt and *p*-eNOS^{Ser1177}/total eNOS; B, Quantification of protein expression by Image Lab. HUVECs were incubated with 100 nmol/L of Akt inhibitor MK2206 for 12 h before treatment with 100 μmol/L HOCl for 24 h. C and D, phosphorylation of *p*-eNOS^{Ser1177}/total eNOS was measured via Western blot and quantified by Image Lab. E, Total Nitric Oxide Assay Kit was used to assess nitrite concentration in cell supernatants of HOCl treatments; F, Total Nitric Oxide Assay Kit was used to assess nitrite concentration in cell supernatants of different treatments. Data are expressed as the mean ± SEM (n = 4 or 6 for each group). An ANOVA and a subsequent Student–Newman–Keuls test were conducted for this figure. $^{**}p < 0.01$, $^{***}p < 0.001$; $^{\#\#}p < 0.01$.

restored endothelium-dependent relaxations, increased NO production in db/db mice. Consistent with the findings of mice, PXDN knockdown also inhibited AGEs-induced endothelial dysfunction in cultured HUVECs. Therefore, we speculate that PXDN may mediates AGEs-induced diabetic vascular endothelial dysfunction.

Previous studies have confirmed that alteration of eNOS activity in the endothelium is one important mechanism of endothelial dysfunction in diabetes [52,53]. The activity of eNOS is mainly regulated by the formation of homodimer, and the post-modification of multisite phosphorylations [54,55]. Among these mechanisms, decreased phosphorylation level in serine 1177 site is believed to have a pivotal role in diabetic endothelial dysfunction [56,57]. In this study, we found that phosphorylation of eNOS on ser1177 was reduced both in thoracic aortas of db/db mice and AGEs-induced HUVECs cells. Moreover, PXDN knockdown significantly improved the reduced eNOS phosphorylation on ser1177, which suggest that PXDN may promote AGEs-mediated diabetic endothelial dysfunction by inhibiting the phosphorylation of eNOS on Ser1177. Akt/protein kinase B (PKB) phosphorylates eNOS at serine 1177, which directly increases eNOS activity [27,58]. Previous studies have found that Akt/eNOS signaling pathways are extensively damaged in diabetes models induced by different pathogenic factors such as insulin resistance and hyperglycemia [59–61]. We further found Akt phosphorylation were impaired by measuring it in thoracic aortas of diabetic mice and HUVECs induced by AGEs. More critically, these injuries were recovered after PXDN knockdown.

We have previously reported that PXDN catalyzes HOCl formation and participates in many pathophysiology of cardiovascular diseases [16,20,62]. In order to further elucidate the specific mechanism of PXDN in endothelial dysfunction, HUVECs were treated with exogenous HOCl. We found that HOCl treatment significantly reduced eNOS

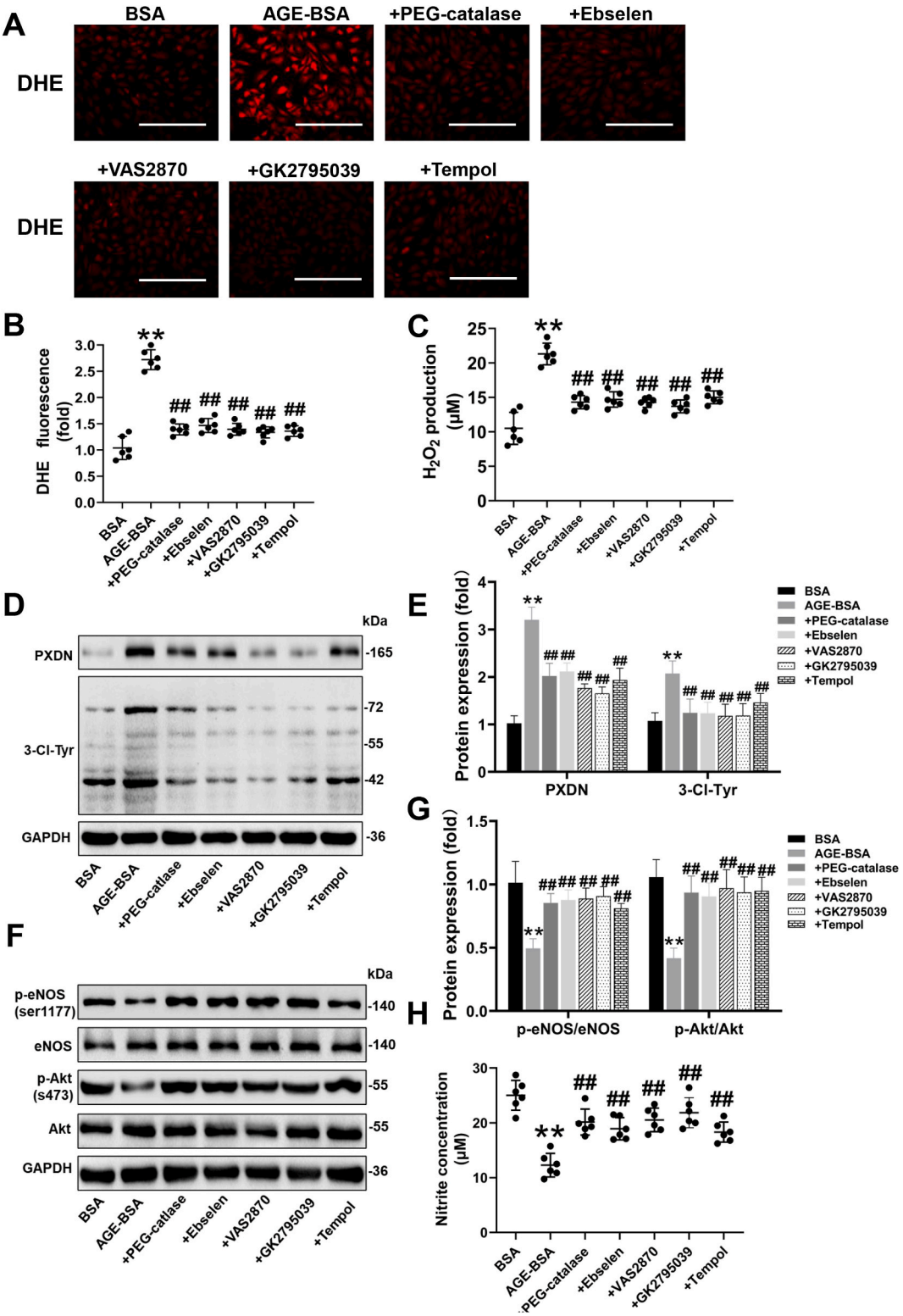

Fig. 6. H_2O_2, ROS scavengers and NOX inhibitors attenuate PXDN-mediated vascular endothelial dysfunction induced by AGEs. Cells were incubated with 400 units PEG-catalase, 40 μM ebselen, 10 μM VAS2870, 25 μM GSK2795039 or 10 μM Tempol for 1 h and then exposed to AGE-BSA (200 μg/mL) for 24 h. A and B, DHE staining and quantification of DHE fluorescence intensity by Image J; C, intracellular H_2O_2 concentration was assessed by Hydrogen Peroxide Assay Kit; D and E, cell expression level of PXDN and 3-Cl-Tyr was measured by Western blot and quantified by Image Lab; F and G, phosphorylation level of *p*-Akt^{Ser473}/total Akt and *p*-eNOS^{Ser1177}/total eNOS was measured by Western blot and quantified by Image Lab; H, nitrite concentration in cell supernatants was measured by Total Nitric Oxide Assay Kit. Bar = 200 μm for DHE staining of HUVECs. Data are expressed as the mean ± SEM (n = 6 for each group). An ANOVA and a subsequent Student–Newman–Keuls test were conducted for this figure. $^{**}p < 0.01$ versus control, $^{\#\#}p < 0.01$ versus AGE-BSA treatment.

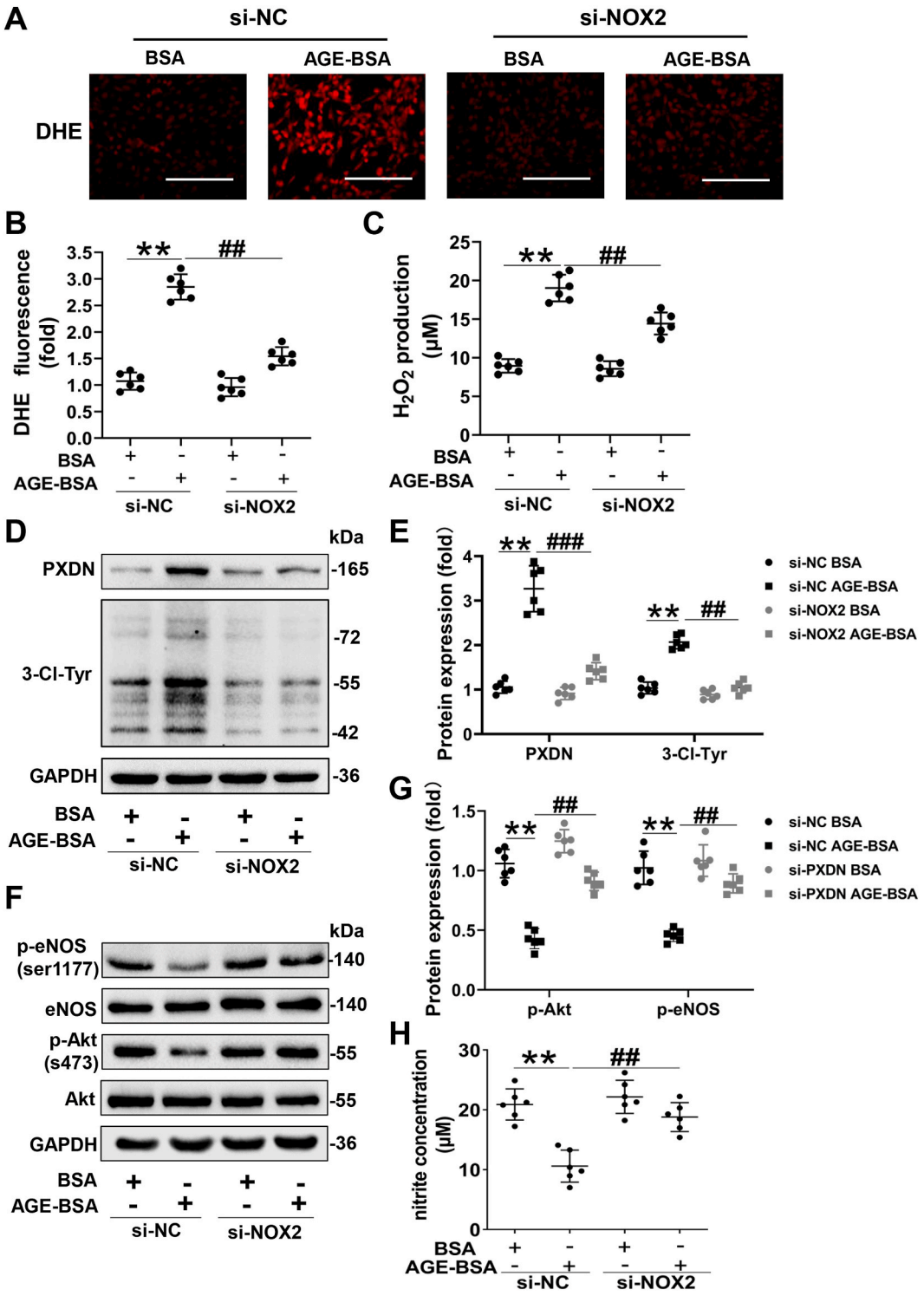

Fig. 7. NOX2 silencing attenuates the effect of AGE-BSA on PXDN and its downstream pathway, restored vascular endothelial function. Cells were transfected with either a negative control siRNA (si-NC) or NOX2 siRNAs (si-NOX2) for 24 h. The medium was then replaced by endothelial cell medium containing 200 μg/mL AGE-BSA for 48 h. A and B, DHE staining and quantification of fluorescence intensity by Image J; C, intracellular H_2O_2 concentration was assessed by Hydrogen Peroxide Assay Kit; D and E, cell expression level of PXDN and 3-Cl-Tyr was measured by Western blot and quantified by Image Lab; F and G, phosphorylation level of *p*-Akt^{Ser473}/total Akt and *p*-eNOS^{Ser1177}/total eNOS was measured by Western blot and quantified by Image Lab; H, nitrite concentration in cell supernatants was measured by Total Nitric Oxide Assay Kit. Bar = 200 μm for DHE staining of HUVECs. Data are expressed as the mean ± SEM (n = 6 for each group). An ANOVA and a subsequent Student–Newman–Keuls test were conducted for this figure. **p < 0.01; $^{\#\#}$P < 0.01, $^{\#\#}$P < 0.001.

phosphorylation on Ser1177 by attenuating Akt phosphorylation, which finally reduced the production of cellular NO. And the Akt inhibitor (MK2206) reduced eNOS phosphorylation and NO level induced by HOCl. These results suggest that HOCl mediated eNOS phosphorylation via activating Akt, leading to NO consumption and AGEs-induced endothelial dysfunction.

Our previously studies have identified PXDN is response to NOX-activated redox signaling [16,18,29]. NOX2 that highly expressed in

endothelial cells is the main source of ROS and plays a critical role in AGEs-induced endothelial dysfunction [11,31,63–65]. In addition to NOX2, other isoforms of NOX (NOX1 and NOX4) are also expressed in vascular tissues, of which NOX1 is mainly expressed in smooth muscle cells and NOX4 is mainly expressed in endothelial cells [66,67]. Excess superoxide production derived from NOX2 and NOX1 in response to diabetic stimulation results in impaired endothelial function, while defining the role of NOX4 has been elusive [68,69]. Some studies suggest that NOX4 may exhibits protective function for decreasing insulin resistance via inhibition of PTP1B [70]. Therefore, NOX2 is considered to be a key enzyme in the NOX family that promotes diabetic endothelial dysfunction. In agreement of these results, we found that protein expression of NOX2 in aortas of db/db mice was significantly higher than that of NOX1 and NOX4. Moreover, NOX2-specific inhibitor significantly reduced ROS production in the aortas and mesenteric arteries of db/db mice compared to non-specific NOX inhibitor and mitochondrial ROS scavenger. Previous studies have found that the NOX2/PXDN pathway is involved in a series of pathophysiological processes including hypoxia-induced vascular remodeling and angiotensin II-induced myocardial hypertrophy [45,71]. Based on the high expression and cellular localization of NOX2 in db/db mice, we hypothesized NOX2 may participates in PXDN-mediated endothelial dysfunction induced by AGEs. We found NOX2 significantly increased in thoracic aortas of db/db mice, which could be suppressed by AGEs breaker. After NOX2 silencing, H_2O_2, ROS scavenger and NOX inhibitors were used to HUVECs, we found that both NOX2 silencing, H_2O_2, ROS scavengers and NOX inhibitors attenuated the AGEs-induced damage on phosphorylation of Akt and eNOS, up-regulating NO level by inhibiting PXDN expression. These results suggest PXDN is a downstream regulator of NOX2 in AGEs-induced endothelial dysfunction.

Here, we firstly showed that PXDN is a mediator in AGEs-induced diabetic vascular endothelial dysfunction via HOCl/Akt/eNOS pathway. We found both PXDN and HOCl could regulate phosphorylation of Akt in diabetic mice and endothelial cells. Admittedly, the mechanism that PXDN regulates Akt phosphorylation remains to be further elucidate. Previous study reported Akt Ser 473 phosphorylation is related to several factors such as mTORC2 Ack1, Src, PTK6, TBK1 and IKBKE [72,73]. Thus, more studies need to be performed to explore the pathway of PXDN-mediated Akt phosphorylation. What is more, to clarify the role of PXDN in AGEs induced diabetic vascular endothelial dysfunction in vivo, endothelium-specific genetically modified animals are needed in the future.

5. Conclusion

To summarize, our results suggested that PXDN may promote AGEs-induced diabetic vascular endothelial dysfunction by attenuating eNOS phosphorylation on Ser1177 via NOX2/HOCl/Akt pathway (Fig. 8). These novel findings suggest a potential target for the early intervention of diabetic vascular disease.

Data availability

All the raw data are available on request from the corresponding authors.

Funding

This work was supported by grants from National Program on Key Basic Research Project of China (Nos. 2019YFF0216304 to S.R.Z.), the National Natural Science Foundation of China of China (No. 81873479 to Z.G.G.), Outstanding Youth Foundation Project of Hunan Natural Science Foundation (Nos. 2019JJ20036 to S.R.Z.), Key R & D Program of Hunan Provincial Department of Science and technology (Nos. 2018SK2137 to S.R.Z.), Chinese Cardiovascular Association V.G foundation (Nos.2017-CCA-VG-005 to S.R.Z).

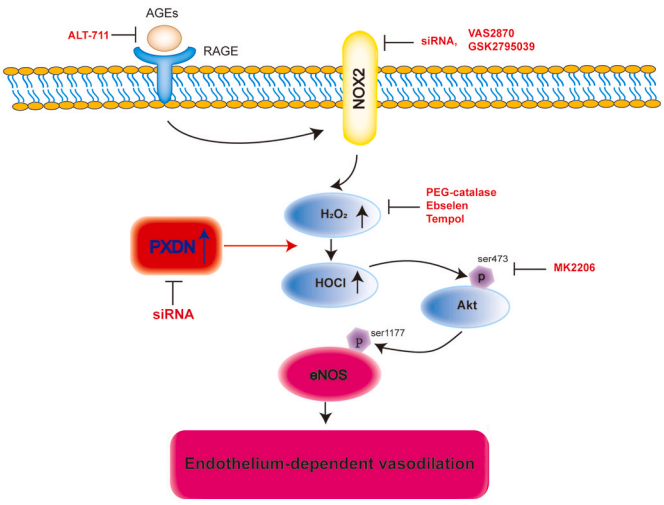

Fig. 8. The proposed pathway by which PXDN mediates AGEs-induced diabetic endothelial dysfunction. AGEs bind their receptor RAGE and subsequently upregulates the expression of NOX2, which is an important source of ROS. This increase in ROS, increases PXDN expression and HOCl production. PXDN-derived HOCl decreases phosphorylation of eNOS on serine 1177 by blocking Akt phosphorylation on serine 473. The decrease of eNOS phosphorylation were found to correlate intimately with endothelial dysfunction.

Contribution statement

Jing Cao, Guogang Zhang, and Ruizheng Shi conceived and designed the study; Jing Cao, Zhaoya Liu, and Qian Xu contributed to data acquisition; Guangjie Cheng and Chan Li analyzed the data; all authors contributed to the writing of this manuscript. Ruizheng Shi is *the guarantor of this work and, as such, had full access to all the data in the study and takes responsibility for the integrity of the data and the accuracy of the data analysis.*

Declaration of competing interest

None.
Authors have no conflict of interest to declare.

Acknowledgement

Authors would like to thank Xiujuan Xia (The Third Xiangya Hospital of Central South University, Changsha, China), Duanfang Liao and Min Fang (Hunan University of Chinese Medicine, Changsha, China) for providing technical assistance and reagents in vascular endothelium relaxtion test.

Appendix A. Supplementary data

Supplementary data to this article can be found online at https://doi.org/10.1016/j.redox.2021.102031.

References

[1] F. Paneni, J.A. Beckman, M.A. Creager, F. Cosentino, Diabetes and vascular disease: pathophysiology, clinical consequences, and medical therapy: part I, Eur. Heart J. 34 (31) (2013) 2436–2443.
[2] J. Xu, M.H. Zou, Molecular insights and therapeutic targets for diabetic endothelial dysfunction, Circulation 120 (13) (2009) 1266–1286.
[3] C.M. Sena, A.M. Pereira, R. Seica, Endothelial dysfunction - a major mediator of diabetic vascular disease, Biochim. Biophys. Acta 1832 (12) (2013) 2216–2231.
[4] G. Targher, A. Lonardo, C.D. Byrne, Nonalcoholic fatty liver disease and chronic vascular complications of diabetes mellitus, Nat. Rev. Endocrinol. 14 (2) (2018) 99–114.

[5] X.L. Du, D. Edelstein, S. Dimmeler, et al., Hyperglycemia inhibits endothelial nitric oxide synthase activity by posttranslational modification at the Akt site, J. Clin. Invest. 108 (9) (2001) 1341–1348.
[6] H. Viswambharan, N.Y. Yuldasheva, A. Sengupta, et al., Selective enhancement of insulin sensitivity in the endothelium in vivo reveals a novel proatherosclerotic signaling loop, Circ. Res. 120 (5) (2017) 784–798.
[7] X. Ren, L. Ren, Q. Wei, et al., Advanced glycation end-products decreases expression of endothelial nitric oxide synthase through oxidative stress in human coronary artery endothelial cells, Cardiovasc. Diabetol. 16 (1) (2017) 52.
[8] A. Goldin, J.A. Beckman, A.M. Schmidt, M.A. Creager, Advanced glycation end products: sparking the development of diabetic vascular injury, Circulation 114 (6) (2006) 597–605.
[9] P.L. Huang, eNOS, metabolic syndrome and cardiovascular disease, Trends Endocrinol. Metabol. 20 (6) (2009) 295–302.
[10] U. Forstermann, W.C. Sessa, Nitric oxide synthases: regulation and function, Eur. Heart J. 33 (7) (2012) 829–837, 837a-837d.
[11] M. Zhang, A.L. Kho, N. Anilkumar, et al., Glycated proteins stimulate reactive oxygen species production in cardiac myocytes: involvement of Nox2 (gp91phox)-containing NADPH oxidase, Circulation 113 (9) (2006) 1235–1243.
[12] R.E. Nelson, L.I. Fessler, Y. Takagi, et al., Peroxidasin: a novel enzyme-matrix protein of Drosophila development, EMBO J. 13 (15) (1994) 3438–3447.
[13] X. Yan, S. Sabrautzki, M. Horsch, et al., Peroxidasin is essential for eye development in the mouse, Hum. Mol. Genet. 23 (21) (2014) 5597–5614.
[14] K. Khan, A. Rudkin, D.A. Parry, et al., Homozygous mutations in PXDN cause congenital cataract, corneal opacity, and developmental glaucoma, Am. J. Hum. Genet. 89 (3) (2011) 464–473.
[15] G. Cheng, J.C. Salerno, Z. Cao, P.J. Pagano, J.D. Lambeth, Identification and characterization of VPO1, a new animal heme-containing peroxidase, Free Radic. Biol. Med. 45 (12) (2008) 1682–1694.
[16] Y.S. Zhang, L. He, B. Liu, et al., A novel pathway of NADPH oxidase/vascular peroxidase 1 in mediating oxidative injury following ischemia-reperfusion, Basic Res. Cardiol. 107 (3) (2012) 266.
[17] H. Peng, L. Chen, X. Huang, et al., Vascular peroxidase 1 up regulation by angiotensin II attenuates nitric oxide production through increasing asymmetrical dimethylarginine in HUVECs, J Am Soc Hypertens 10 (9) (2016) 741–751, e3.
[18] R. Shi, C. Hu, Q. Yuan, et al., Involvement of vascular peroxidase 1 in angiotensin II-induced vascular smooth muscle cell proliferation, Cardiovasc. Res. 91 (1) (2011) 27–36.
[19] E. Lazar, Z. Peterfi, G. Sirokmany, et al., Structure-function analysis of peroxidasin provides insight into the mechanism of collagen IV crosslinking, Free Radic. Biol. Med. 83 (2015) 273–282.
[20] B. You, Y. Liu, J. Chen, et al., Vascular peroxidase 1 mediates hypoxia-induced pulmonary artery smooth muscle cell proliferation, apoptosis resistance and migration, Cardiovasc. Res. 114 (1) (2018) 188–199.
[21] H. Peng, K. Zhang, Z. Liu, et al., VPO1 modulates vascular smooth muscle cell phenotypic switch by activating extracellular signal-regulated kinase 1/2 (ERK 1/2) in abdominal aortic aneurysms, J Am Heart Assoc 7 (17) (2018), e010069.
[22] W.S. Cheang, W.T. Wong, X.Y. Tian, et al., Endothelial nitric oxide synthase enhancer reduces oxidative stress and restores endothelial function in db/db mice, Cardiovasc. Res. 92 (2) (2011) 267–275.
[23] W.T. Wong, X.Y. Tian, A. Xu, et al., Angiotensin II type 1 receptor-dependent oxidative stress mediates endothelial dysfunction in type 2 diabetic mice, Antioxidants Redox Signal. 13 (6) (2010) 757–768.
[24] Y. Zhang, J. Liu, X.Y. Tian, et al., Inhibition of bone morphogenic protein 4 restores endothelial function in db/db diabetic mice, Arterioscler. Thromb. Vasc. Biol. 34 (1) (2014) 152–159.
[25] C. Yang, M.A. Talukder, S. Varadharaj, M. Velayutham, J.L. Zweier, Early ischaemic preconditioning requires Akt- and PKA-mediated activation of eNOS via serine1176 phosphorylation, Cardiovasc. Res. 97 (1) (2013) 33–43.
[26] V. Garcia-Morales, M. Luaces-Regueira, M. Campos-Toimil, The cAMP effectors PKA and Epac activate endothelial NO synthase through PI3K/Akt pathway in human endothelial cells, Biochem. Pharmacol. 145 (2017) 94–101.
[27] S. Zhang, S. Guo, X.B. Gao, et al., Matrine attenuates high-fat diet-induced in vivo and ox-LDL-induced in vitro vascular injury by regulating the PKCalpha/eNOS and PI3K/Akt/eNOS pathways, J. Cell Mol. Med. 23 (4) (2019) 2731–2743.
[28] H. Li, Z. Cao, G. Zhang, V.J. Thannickal, G. Cheng, Vascular peroxidase 1 catalyzes the formation of hypohalous acids: characterization of its substrate specificity and enzymatic properties, Free Radic. Biol. Med. 53 (10) (2012) 1954–1959.
[29] Y.P. Bai, C.P. Hu, Q. Yuan, et al., Role of VPO1, a newly identified heme-containing peroxidase, in ox-LDL induced endothelial cell apoptosis, Free Radic. Biol. Med. 51 (8) (2011) 1492–1500.
[30] N.X. Chen, S. Srinivasan, K. O'Neill, et al., Effect of advanced glycation end-products (AGE) lowering drug ALT-711 on biochemical, vascular, and bone parameters in a rat model of CKD-MBD, J. Bone Miner. Res. 35 (3) (2020) 608–617.
[31] F. Giacco, M. Brownlee, Oxidative stress and diabetic complications, Circ. Res. 107 (9) (2010) 1058–1070.
[32] A. Patel, S. MacMahon, J. Chalmers, et al., Intensive blood glucose control and vascular outcomes in patients with type 2 diabetes, N. Engl. J. Med. 358 (24) (2008) 2560–2572.
[33] H.C. Gerstein, M.E. Miller, R.P. Byington, et al., Effects of intensive glucose lowering in type 2 diabetes, N. Engl. J. Med. 358 (24) (2008) 2545–2559.
[34] R.G. Dluhy, G.T. McMahon, Intensive glycemic control in the ACCORD and ADVANCE trials, N. Engl. J. Med. 358 (24) (2008) 2630–2633.
[35] S.I. Yamagishi, N. Nakamura, T. Matsui, Glycation and cardiovascular disease in diabetes: a perspective on the concept of metabolic memory, J. Diabetes 9 (2) (2017) 141–148.
[36] S. Yamagishi, K. Nakamura, T. Imaizumi, Advanced glycation end products (AGEs) and diabetic vascular complications, Curr. Diabetes Rev. 1 (1) (2005) 93–106.
[37] C. Zhang, J. Yang, L.K. Jennings, Leukocyte-derived myeloperoxidase amplifies high-glucose–induced endothelial dysfunction through interaction with high-glucose–stimulated, vascular non–leukocyte-derived reactive oxygen species, Diabetes 53 (11) (2004) 2950–2959.
[38] R. Tian, Y. Ding, Y.Y. Peng, N. Lu, Myeloperoxidase amplified high glucose-induced endothelial dysfunction in vasculature: role of NADPH oxidase and hypochlorous acid, Biochem. Biophys. Res. Commun. 484 (3) (2017) 572–578.
[39] G. Bhave, C.F. Cummings, R.M. Vanacore, et al., Peroxidasin forms sulfilimine chemical bonds using hypohalous acids in tissue genesis, Nat. Chem. Biol. 8 (9) (2012) 784–790.
[40] T.T. Li, Y.S. Zhang, L. He, et al., Inhibition of vascular peroxidase alleviates cardiac dysfunction and apoptosis induced by ischemia-reperfusion, Can. J. Physiol. Pharmacol. 90 (7) (2012) 851–862.
[41] G. Cheng, H. Li, Z. Cao, et al., Vascular peroxidase-1 is rapidly secreted, circulates in plasma, and supports dityrosine cross-linking reactions, Free Radic. Biol. Med. 51 (7) (2011) 1445–1453.
[42] H. Li, Z. Cao, D.R. Moore, et al., Microbicidal activity of vascular peroxidase 1 in human plasma via generation of hypochlorous acid, Infect. Immun. 80 (7) (2012) 2528–2537.
[43] R. Shi, Z. Cao, H. Li, et al., Peroxidasin contributes to lung host defense by direct binding and killing of gram-negative bacteria, PLoS Pathog. 14 (5) (2018), e1007026.
[44] Y. Tang, Q. Xu, H. Peng, et al., The role of vascular peroxidase 1 in ox-LDL-induced vascular smooth muscle cell calcification, Atherosclerosis 243 (2) (2015) 357–363.
[45] W. Yang, Z. Liu, Q. Xu, et al., Involvement of vascular peroxidase 1 in angiotensin II-induced hypertrophy of H9c2 cells, J Am Soc Hypertens 11 (8) (2017) 519–529, e1.
[46] E.L. Wang, M.M. Jia, F.M. Luo, et al., Coordination between NADPH oxidase and vascular peroxidase 1 promotes dysfunctions of endothelial progenitor cells in hypoxia-induced pulmonary hypertensive rats, Eur. J. Pharmacol. 857 (2019) 172459.
[47] Y.Z. Zhang, L. Wang, J.J. Zhang, et al., Vascular peroxide 1 promotes ox-LDL-induced programmed necrosis in endothelial cells through a mechanism involving beta-catenin signaling, Atherosclerosis 274 (2018) 128–138.
[48] S.Y. Liu, Q. Yuan, X.H. Li, et al., Role of vascular peroxidase 1 in senescence of endothelial cells in diabetes rats, Int. J. Cardiol. 197 (2015) 182–191.
[49] L. Ge, G. Zhang, B. You, et al., The role of losartan in preventing vascular remodeling in spontaneously hypertensive rats by inhibition of the H2O2/VPO1/HOCl/MMPs pathway, Biochem. Biophys. Res. Commun. 493 (1) (2017) 855–861.
[50] Y. Tang, Q. Xu, H. Peng, et al., The role of vascular peroxidase 1 in ox-LDL-induced vascular smooth muscle cell calcification, Atherosclerosis 243 (2) (2015) 357–363.
[51] Z. Liu, Y. Liu, Q. Xu, et al., Critical role of vascular peroxidase 1 in regulating endothelial nitric oxide synthase, Redox Biol 12 (2017) 226–232.
[52] Y. Shi, P.M. Vanhoutte, Macro- and microvascular endothelial dysfunction in diabetes, J. Diabetes 9 (5) (2017) 434–449.
[53] S.B. Chandra, S. Mohan, B.M. Ford, et al., Targeted overexpression of endothelial nitric oxide synthase in endothelial cells improves cerebrovascular reactivity in Ins2Akita-type-1 diabetic mice, J. Cerebr. Blood Flow Metabol. 36 (6) (2016) 1135–1142.
[54] U. Forstermann, W.C. Sessa, Nitric oxide synthases: regulation and function, Eur. Heart J. 33 (7) (2012) 829–837, 837a-837d.
[55] P.W. Shaul, Regulation of endothelial nitric oxide synthase: location, location, location, Annu. Rev. Physiol. 64 (2002) 749–774.
[56] M. Siragusa, J.A. Oliveira, P.F. Malacarne, et al., VE-PTP inhibition elicits eNOS phosphorylation to blunt endothelial dysfunction and hypertension in diabetes, Cardiovasc. Res. 117 (6) (2021) 1546–1556.
[57] X. Ren, L. Ren, Q. Wei, et al., Advanced glycation end-products decreases expression of endothelial nitric oxide synthase through oxidative stress in human coronary artery endothelial cells, Cardiovasc. Diabetol. 16 (1) (2017) 52.
[58] J.Y. Li, W.Q. Huang, R.H. Tu, et al., Resveratrol rescues hyperglycemia-induced endothelial dysfunction via activation of Akt, Acta Pharmacol. Sin. 38 (2) (2017) 182–191.
[59] Y. Horio, Diabetes: insulin signal meets SIRT1 at AKT, Nat. Rev. Endocrinol. 8 (3) (2011) 131–132.
[60] K.Y. Howangyin, J.S. Silvestre, Diabetes mellitus and ischemic diseases: molecular mechanisms of vascular repair dysfunction, Arterioscler. Thromb. Vasc. Biol. 34 (6) (2014) 1126–1135.
[61] X. Huang, G. Liu, J. Guo, Z. Su, The PI3K/AKT pathway in obesity and type 2 diabetes, Int. J. Biol. Sci. 14 (11) (2018) 1483–1496.
[62] Z. Liu, Q. Xu, Q. Yang, et al., Vascular peroxidase 1 is a novel regulator of cardiac fibrosis after myocardial infarction, Redox Biol 22 (2019), 101151.
[63] M.P. Wautier, O. Chappey, S. Corda, et al., Activation of NADPH oxidase by AGE links oxidant stress to altered gene expression via RAGE, Am. J. Physiol. Endocrinol. Metab. 280 (5) (2001) E685–E694.
[64] C. Petersen, D. Bharat, B.R. Cutler, et al., Circulating metabolites of strawberry mediate reductions in vascular inflammation and endothelial dysfunction in db/db mice, Int. J. Cardiol. 263 (2018) 111–117.
[65] J. Su, P.A. Lucchesi, R.A. Gonzalez-Villalobos, et al., Role of advanced glycation end products with oxidative stress in resistance artery dysfunction in type 2 diabetic mice, Arterioscler. Thromb. Vasc. Biol. 28 (8) (2008) 1432–1438.
[66] B. Lassegue, D. Sorescu, K. Szocs, et al., Novel gp91(phox) homologues in vascular smooth muscle cells: nox1 mediates angiotensin II-induced superoxide formation and redox-sensitive signaling pathways, Circ. Res. 88 (9) (2001) 888–894.

[67] T. Ago, T. Kitazono, H. Ooboshi, et al., Nox4 as the major catalytic component of an endothelial NAD(P)H oxidase, Circulation 109 (2) (2004) 227–233.
[68] P. Sukumar, H. Viswambharan, H. Imrie, et al., Nox2 NADPH oxidase has a critical role in insulin resistance-related endothelial cell dysfunction, Diabetes 62 (6) (2013) 2130–2134.
[69] S.P. Gray, E. Di Marco, J. Okabe, et al., NADPH oxidase 1 plays a key role in diabetes mellitus-accelerated atherosclerosis, Circulation 127 (18) (2013) 1888–1902.
[70] G.D. Frank, S. Eguchi, E.D. Motley, The role of reactive oxygen species in insulin signaling in the vasculature, Antioxidants Redox Signal. 7 (7–8) (2005) 1053–1061.
[71] E.L. Wang, M.M. Jia, F.M. Luo, et al., Coordination between NADPH oxidase and vascular peroxidase 1 promotes dysfunctions of endothelial progenitor cells in hypoxia-induced pulmonary hypertensive rats, Eur. J. Pharmacol. 857 (2019), 172459.
[72] P. Abeyrathna, Y. Su, The critical role of Akt in cardiovascular function, Vasc. Pharmacol. 74 (2015) 38–48.
[73] X. Huang, G. Liu, J. Guo, Z. Su, The PI3K/AKT pathway in obesity and type 2 diabetes, Int. J. Biol. Sci. 14 (11) (2018) 1483–1496.